HHS Public Access

Author manuscript

Sci Transl Med. Author manuscript; available in PMC 2018 December 16.

Published in final edited form as:

Sci Transl Med. 2015 March 18; 7(279): 279ra38. doi:10.1126/scitranslmed.3010841.

A microRNA-Hippo pathway that promotes cardiomyocyte proliferation and cardiac regeneration in mice

Ying Tian[1,2,*], **Ying Liu**[1], **Tao Wang**[1], **Ning Zhou**[1,3], **Jun Kong**[1], **Li Chen**[1], **Melinda Snitow**[1], **Michael Morley**[1], **Deqiang Li**[1], **Nataliya Petrenko**[1,2], **Su Zhou**[1], **Minmin Lu**[1], **Erhe Gao**[2], **Walter J. Koch**[2], **Kathleen M. Stewart**[1], and **Edward E. Morrisey**[1,4,5,6,*]

[1]Department of Medicine, University of Pennsylvania, Philadelphia, PA 19104, USA.

[2]Department of Pharmacology, Center for Translational Medicine, Temple University School of Medicine, Philadelphia, PA 19140, USA.

[3]Department of Ultrasound Diagnostics, Tangdu Hospital, Fourth Military Medical University, Xi'an 710038, China.

[4]Department of Cell and Developmental Biology, University of Pennsylvania, Philadelphia, PA19104, USA.

[5]Institute for Regenerative Medicine, University of Pennsylvania, Philadelphia, PA 19104, USA.

[6]Cardiovascular Institute, University of Pennsylvania, Philadelphia, PA 19104, USA.

Abstract

In contrast to lower vertebrates, the mammalian heart has limited capacity to regenerate after injury in part due to ineffective reactivation of cardiomyocyte proliferation. We show that the

[*]Corresponding author. ying.tian@temple.edu (Y.T.); emorrise@mail.med.upenn.edu (E.E.M.).

Author contributions: Y.T. planned and managed the majority of experiments and helped write the manuscript. Y.L. performed cultured cell experiments and generated mouse lines. T.W. and L.C. performed all the animal surgeries. N.Z. performed echo studies. J.K. assisted with intravenous injections. M.S. performed in vitro experiments. M.M. assisted with bioinformatics. D.L. helped with FACS analysis and interpretation of the data. N.P. performed adult cardiomyocyte isolation. S.Z. and M.L. assisted with histology. E.G. and W.J.K. helped with MI experiments. K.M.S. helped manage the experiments. E.E.M. supervised all experiments and wrote the manuscript.

Competing interests: The authors declare that they have no competing interests.

Data and materials availability: Complete microarray data set has been deposited in the Gene Expression Omnibus database (accession # GSE54988).

SUPPLEMENTARY MATERIALS

www.sciencetranslationalmedicine.org/cgi/content/full/7/279/279ra38/DC1

microRNA cluster miR302–367 is important for cardiomyocyte proliferation during development and is sufficient to induce cardiomyocyte proliferation in the adult and promote cardiac regeneration. In mice, loss of miR302–367 led to decreased cardiomyocyte proliferation during development. In contrast, increased miR302–367 expression led to a profound increase in cardiomyocyte proliferation, in part through repression of the Hippo signal transduction pathway. Postnatal reexpression of miR302–367 reactivated the cell cycle in cardiomyocytes, resulting in reduced scar formation after experimental myocardial infarction. However, long-term expression of miR302–367 induced cardiomyocyte dedifferentiation and dysfunction, suggesting that persistent reactivation of the cell cycle in postnatal cardiomyocytes is not desirable. This limitation can be overcome by transient systemic application of miR302–367 mimics, leading to increased cardiomyocyte proliferation and mass, decreased fibrosis, and improved function after injury. Our data demonstrate the ability of microRNA-based therapeutic approaches to promote mammalian cardiac repair and regeneration through the transient activation of cardiomyocyte proliferation.

INTRODUCTION

Although cardiomyocytes derived from pluripotent stem cells have been proposed as a therapeutic approach to replace myocardium lost after injury or disease, efficient engraftment and survival of the exogenous cells remain a major challenge. An alternative approach is to regenerate cardiomyocytes in situ through activation of cardiomyocyte proliferation. Until recently, the adult mammalian heart has been considered a terminally differentiated organ with limited capacity to regenerate after injury (1). However, recent evidence has shown that the neonatal heart can regenerate through increased cardiomyocyte proliferation (2, 3). This ability to regenerate in response to injury ends by 7 days after birth in mice, corresponding to the exit of cardiomyocytes from the cell cycle. Although there is some evidence for a very low level of postnatal cardiomyocyte proliferation, which can be increased after injury (4), it is insufficient to replenish lost cardiomyocytes after injury and reestablish proper heart function.

One important hurdle for cardiomyocytes to overcome in reentering the cell cycle is the rigidity of the sarcomere structure, which must be disassembled for cytokinesis to occur. Such disassembly may require signals for cardiomyocyte dedifferentiation, which is accompanied by multiple cellular changes including reactivation of gene expression programs restricted to the embryonic state. Thus, approaches that reactivate or increase postnatal cardiomyocyte proliferation could have a positive effect on cardiac repair and regeneration, but their persistence would need to be carefully tuned to avoid cardiomyocyte dysfunction associated with a highly proliferative, dedifferentiated state.

MicroRNAs (miRNAs) can have potent effects on gene expression and can alter cell phenotype by coordinately targeting multiple components in important cellular pathways (5). Several miRNA clusters or families are expressed in early mouse development and play important roles in maintaining tissue-specific progenitor identity. One such cluster, miR302–367, is expressed during early embryogenesis in embryonic stem (ES) cells and in the developing lung endoderm, where it promotes a dedifferentiated phenotype characterized by high levels of cell proliferation and reduced levels of differentiation markers (6–8).

Here, we demonstrate that miR302–367 is expressed in early mouse cardiac development and is important for cardiomyocyte proliferation during embryonic development. Increased miR302–367 expression led to high-level and persistent cardiomyocyte proliferation and ultimately cardiomegaly. miR302–367 functions, in part, by targeting several components of the Hippo signal transduction pathway. Persistent reexpression of miR302–367 in the postnatal heart reactivated the cardiomyocyte cell cycle and increased cardiomyocyte number and regeneration but led to prolonged induction of an immature dedifferentiated state and heart failure. In contrast, transient treatment of mice with miR302–367 mimics promoted mouse cardiac regeneration without the adverse effects on physiological function. Thus, our studies suggest that an miRNA mimic approach could be harnessed therapeutically to promote cardiomyocyte proliferation and cardiac regeneration without the deleterious effects of persistent dedifferentiation and physiological dysfunction.

RESULTS

miR302–367 cluster is important for cardiomyocyte proliferation during development

Expression of miR302–367 during early lung development in mice (7) suggests that this miRNA cluster may be expressed in other tissues during development. To determine whether the miR302–367 cluster was expressed during cardiac development, we performed quantitative real-time PCR (qRT-PCR) on RNA isolated from mouse embryonic hearts at multiple developmental stages. All five members of the miR302–367 cluster were expressed at embryonic day (E) 9.5, but their expression decreased significantly after E11.5 (Fig. 1A). In situ hybridization indicated that the miR302–367 cluster is expressed in the myocardium of the embryonic mouse heart as early as E8.5 (fig. S1A). At postnatal and adult stages, the expression of these miRNAs was not detectable by qRT-PCR (Fig. 1A).

To investigate the role of the miR302–367 cluster in heart development, we generated a miR302–367$^{flox/flox}$ mouse line and used the Nkx2.5^{cre} line to delete the entire cluster during cardiogenesis (9) (fig. S1, B and C). Decreased expression of members of the miR302–367 cluster was observed in Nkx2.5^{cre}:miR302–367$^{flox/flox}$ hearts by qRT-PCR (fig. S1D). The miR302–367 cluster is located in intron 8 of the *Larp7* gene (6). However, the expression of *Larp7* was unaffected by genetic deletion of the miR302–367 locus (fig. S1E). Nkx2.5^{cre}:miR302–367$^{flox/flox}$ hearts exhibited thinner ventricular walls and decreased proliferation compared with control littermates (Fig. 1, B and C).

Decreased expression of the cell cycle proliferation gene *Ccnd1* (cyclin D1) was consistent with decreased cell proliferation in Nkx2.5^{cre}:miR302–367$^{flox/flox}$ mutant hearts (Fig. 1D). Moreover, Nkx2.5^{cre}:miR302–367$^{flox/flox}$ mutant hearts showed decreased expression of *Gata4*, *Nkx2.5*, *Myh6*, and *Myh7*, indicating defects in cardiomyocyte differentiation at E14.5 (Fig. 1D). However, we did not observe a significant change in programmed cell death or loss in viability in Nkx2.5^{cre}:miR302–367$^{flox/flox}$ mutants (fig. S1F), suggesting compensation by other miRNAs or pathways later in development.

Overexpression of miR302–367 promotes cardiomyocyte proliferation in embryonic and postnatal hearts

We generated a conditional mouse line to perform miR302–367 gain-of-function experiments in vivo (R26R-miR302–367$^{Tg/+}$) (fig. S2, A andB) (10). Activating this allele using the Nkx2.5^{cre} line resulted in high-level expression of all members of the miR302–367 cluster (fig. S2C) and a marked increase in cardiomyocyte proliferation at E18.5 (Fig. 2A). Nkx2.5^{cre}:R26R-miR302–367$^{Tg/+}$ mutants died by P28. At P20, Nkx2.5^{cre}:R26R-miR302–367$^{Tg/+}$ mutants exhibited profound cardiac enlargement, or cardiomegaly, accompanied by extensive cardiomyocyte proliferation (Fig. 2B). This is in contrast to control littermates, which did not exhibit noticeable cardiomyocyte proliferation at P20, consistent with previous observations (11–13).

We isolated cardiomyocytes from P17 hearts and found a significant increase in the percentage of mononucleated and binucleated cardiomyocytes and a decrease in the percentage of multinucleated cardiomyocytes (fig. S2D), suggesting that miR302–367 overexpression affects both cell cycle activity and nucleation of cardiomyocytes when expressed from the beginning of cardiac development. Although heart weight–to–tibia length ratios were significantly higher for Nkx2.5^{cre}:R26R-miR302–367$^{Tg/+}$ mutants at P20 (fig. S2E), cardiomyocytes in these mutants were smaller and exhibited disorganized sarcomeric structure compared to control cardiomyocytes, suggesting increased cardiomyocyte number and a less mature phenotype (Fig. 3A and fig. S2F). Nkx2.5^{cre}:R26R-miR302–367$^{Tg/+}$ mutant hearts had poor cardiac function with reduced ejectionfractionand fractional shortening (fig. S2G). Cardiomyocyte apoptosis was increased in Nkx2.5^{cre}:R26R-miR302–367$^{Tg/+}$ hearts at P20 compared with littermate control Nkx2.5^{cre} hearts, but this may have been due to the overall defects in cardiomyocyte maturation, which led to compromised cardiac function and failure (fig. S2H).

To better understand the effects that overexpression of miR302–367 has on the cardiomyocyte transcriptome, we performed microarray analysis on ventricles from Nkx2.5^{cre}:R26R-miR302–367$^{Tg/+}$ P14 mutant and control hearts. Gene ontology analysis revealed that the most differentially modulated genes in Nkx2.5^{cre}:R26R-miR302–367$^{Tg/+}$ hearts belonged to pathways involved in the control of cell proliferation and negative regulation of cell differentiation (Fig. 3B). qRT-PCR confirmed increased expression of a variety of cell proliferation–associated genes, including *Brca2*, *RacGap1*, *Nusap1*, *Myh10*, and *Cks2*, compared with Nkx2.5^{cre} hearts (Fig. 3C), in addition to increased expression of *Bcl2*, which is a repressor of apoptosis, and several markers associated with negative regulation of cardiomyocyte differentiation, including *Myh7*, *c-Kit*, and *Nppa* (Fig. 3, D and E) (14, 15). Expression of *Myh6* was unaffected by miR302–367 over-expression (Fig. 3E). Overexpression of miR302–367 in developing cardiomyocytes therefore led to a highly proliferative, immature dedifferentiated phenotype in cardiomyocytes.

In contrast, miR302–367 overexpression resulted in down-regulation of programmed cell death (Fig. 3D). We also observed that miR302–367 overexpression resulted in down-regulation of fatty acid metabolism genes including *PparA*, *PparD*, and *Acox1*, suggesting cardiomyocyte dysfunction (Fig. 3F). Together, these data demonstrate increased proliferation and inhibition of maturation of cardiomyocytes in Nkx2.5^{cre}:R26R-miR302–

$367^{Tg/+}$ mutants, indicating that persistent overexpression of miR302–367 leads to a dedifferentiated cardiomyocyte phenotype and compromised cardiac function.

miR302–367 inhibits the Hippo pathway to promote cardiomyocyte proliferation

To further identify miR302–367 target genes, we performed high-throughput sequencing of RNA isolated by cross-linking immunoprecipitation (HITS-CLIP) with argonaute-2/miRNA:mRNA complexes. Mouse ES cells were used given the high level of miR302–367 expression in these cells (16). Using a stringent cutoff of 100 reads per million (RPM), we detected 51 miRNAs including members of miR302–367 (table S1). We compared the identified mRNA targets from HITS-CLIP with all possible predictions of miRNA/mRNA targeting relationships obtained from miRanda (17). The overlap set contained 48 genes, many of which were associated with the regulation of cell cycle and apoptosis (fig. S3A and table S2).

In our HITS-CLIP data, miR-302 targeted sequences in the 3′ untranslated region (3′UTR) of Mst1 (Stk4), a core component of Hippo signaling kinase cascade (table S3). Moreover, miRanda predicted that Lats2 and Mob1b, essential kinases in the Hippo pathway, were potential targets of miR302. The Hippo signal transduction pathway regulates organ size and cell proliferation, and loss of Mst1/2 and Lats kinases in the developing mouse heart causes increased proliferation in cardiomyocytes (18). Thus, we hypothesized that miR302–367 regulates cardiomyocyte proliferation through the inhibition of Hippo signaling.

To verify changes in expression of Hippo components mediated by loss and gain of miR302–367 function, we performed qRT-PCR and Western blots on $Nkx2.5^{cre}$:$miR302–367^{flox/flox}$ and $Nkx2.5^{cre}$:R26R-$miR302–367^{Tg/+}$ hearts. These data revealed that overexpression of miR302–367 led to decreased expression of *Mst1*, *Lats2*, and *Mob1b*, whereas loss of miR302–367 expression led to increased expression of these genes (Fig. 4A and fig. S3, B and C). Expression of miR302–367 also led to decreased activity of luciferase reporters for the 3′UTRs of Mst1, Lats2, and Mob1b, and mutation of the miR302–367 binding sites abrogated this repression (Fig. 4B and fig. S3D). These findings suggest that miR302–367 inhibits Hippo pathway activity through repression of the kinases Mst1, Lats2, and Mob1b.

Yes activated protein (Yap) is the downstream transcriptional effector of Hippo signaling (19). Phosphorylated Yap (phospho-Yap) normally resides in the cytoplasm and is transcriptionally inactive. Upon loss of Hippo signaling, Yap is translocated to the nucleus where it binds to members of the TEAD transcription factor family and activates gene expression, including pathways that promote proliferation and survival (19). Overexpression of a transcriptionally active form of Yap (YapS127A) in the mouse heart promotes cardiomyocyte proliferation and cardiac re generation (20–22). To determine whether overexpression of miR302–367 affected Yap phosphorylation and activity, we examined the expression of Yap and phospho-Yap in $Nkx2.5^{cre}$:R26R-$miR302–367^{Tg/+}$ hearts. Cardiomyocytes of control hearts at E18.5 exhibited diffuse cytoplasmic location of phospho-Yap (Fig. 4C). $Nkx2.5^{cre}$:R26R-$miR302–367^{Tg/+}$ hearts showed reduced phospho-Yap expression. By contrast, immunostaining for total Yap revealed an increase in nuclear Yap in $Nkx2.5^{cre}$:R26R-$miR302–367^{Tg/+}$ hearts (Fig. 4C). Loss of miR302–367 expression

also led to enhanced Yap phosphorylation, but decreased nuclear Yap expression, in the developing myocardium of Nkx2.5^{cre}:miR302–367$^{flox/flox}$ hearts at E10.5 (fig. S3E).

To investigate whether miR302–367 regulation of Hippo signaling was responsible, at least in part, for the increased proliferation observed in cardiomyocytes of Nkx2.5^{cre}:R26R-miR302–367$^{Tg/+}$ hearts, Yap expression was inhibited using short hairpin RNAs (shRNAs) in the presence of miR302–367 expression in isolated neonatal mouse cardiomyocytes. Lentiviral overexpression of miR302–367 resulted in increased neonatal cardiomyocyte proliferation (Fig. 4D). shRNA-mediated inhibition of Yap resulted in decreased proliferation caused by miR302–367 overexpression (Fig. 4D and fig. S3F).

We also examined the effects of individual miR-302 family members on cardiomyocyte proliferation. Treatment of mouse neonatal cardiomyocytes with a miR302b mimic led to an increased number of Ki67^{+}/cardiac Troponin T (cTnT)$^{+}$ cardiomyocytes, whereas miR302c mimics did not induce a similar significant increase in proliferation (fig. 3G). The use of both miR302b and miR302c mimics led to an additive increase in cardiomyocyte proliferation, greater than that with either mimic alone (fig. S3G). Together, these data demonstrate that miR302–367 targets multiple components of the Hippo signal transduction pathway to promote cardiomyocyte proliferation, as illustrated in the schematic in Fig. 4E.

miR302–367 promotes adult cardiac regeneration after myocardial infarction through increased cardiomyocyte proliferation

We next examined whether conditional overexpression of miR302–367 in the adult heart could reactivate cardiomyocyte proliferation. We generated Myh6^{mercremer}:R26R-miR302–367$^{Tg/+}$ animals to specifically overexpress miR302–367 in cardiomyocytes in the adult heart. qRT-PCR confirmed high-level expression of all members of the miR302–367 cluster after tamoxifen administration (fig. S4A and table S4). Eight days after the start of tamoxifen treatment, the cardiomyocytes in Myh6^{mercremer}: R26R-miR302–367$^{Tg/+}$ hearts reentered the cell cycle (Fig. 5, A and B). The number of cardiomyocytes undergoing mitosis (PH3^{+}) and cytokinesis (Aurora B kinase^{+}) was also increased in Myh6^{mercremer}:R26R-miR302–367$^{Tg/+}$ hearts (Fig. 5, C and D), paralleled by a reduction in apoptosis (fig. S4B).

The heart weight–to–tibia length ratio increased in Myh6^{mercremer}:R26R-miR302–367$^{Tg/+}$ animals 2 weeks after initiation of miR302–367 overexpression (fig. S4C). The total number of cardiomyocytes as well as the percentage of mononucleated cardiomyocytes increased after 2 weeks (Fig. 5, E and F). The size of cardiomyocytes in Myh6^{mercremer}:R26R-miR302–367$^{Tg/+}$ heart was also smaller compared to control cardiomyocytes (Fig. 5G). The expression of genes associated with cell proliferation, including *Cks2* and *Ccnd1*, increased in Myh6^{mercremer}:R26R-miR302–367$^{Tg/+}$ hearts (fig. S4D). In contrast, the expression of genes associated with Hippo signaling components and programmed cell death decreased in Myh6^{mercremer}:R26R-miR302–367$^{Tg/+}$ mutants (fig. S4D). miR302–367 overexpression in the adult heart therefore resulted in cardiomyocyte cell cycle reactivation.

To determine whether ectopic expression of miR302–367 can promote cardiac regeneration in adult mice, we performed LAD ligation—inducing a myocardial infarction (MI)—on

Myh6^{mercremer}:R26R-miR302–367$^{Tg/+}$ and control Myh6^{mercremer} mice (Fig. 6A). Three weeks after injury, Myh6^{mercremer} hearts exhibited extensive fibrotic scarring and loss of myocardial tissue, whereas Myh6^{mercremer}:R26R-miR302–367$^{Tg/+}$ hearts had significantly reduced fibrotic scarring with an increase in myocardial tissue (Fig. 6, B and C). Immunostaining showed reduced expression of phospho-Yap, but enhanced expression of nuclear Yap, in Myh6^{mercremer}:R26R-miR302–367$^{Tg/+}$ hearts compared to Myh6^{mercremer} hearts (fig. S5A). Moreover, the number of PH3^{+} cardiomyocytes was significantly higher in Myh6^{mercremer}:R26R-miR302–367$^{Tg/+}$ hearts than in Myh6^{mercremer} controls 3 weeks after injury (Fig. 6D). These data indicate that expression of miR302–367 in the adult heart can promote cardiomyocyte proliferation, which contributes to reduced post-injury fibrotic scarring.

Despite these intriguing findings, we found that Myh6^{mercremer}:R26R-miR302–367$^{Tg/+}$ hearts exhibited ventricular dilation and a reduction in fractional shortening and ejection fraction 3 weeks after injury (Fig. 6E). We hypothesized that sustained cardiomyocyte proliferation in the adult heart caused by prolonged miR302–367 overexpression compromised cardiac function, possibly by inducing a persistent dedifferentiated and highly proliferative phenotype. We examined the expression of genes associated with cardiomyocyte proliferation and differentiation at days 10 and 21 after miR302–367 overexpression. There was a persistent up-regulation of *Cks2*, a marker for cell proliferation, at both time points in Myh6^{mercremer}:R26R-miR302–367$^{Tg/+}$ hearts (fig. S5B). In contrast, we observed the persistent down-regulation in the ratio of *Myh6* (α-myosin heavy chain) to *Myh7* (β-myosin heavy chain), a marker for fetal gene activation in the rodent hearts that is associated with cardiac dysfunction and failure (23), in Myh6^{mercremer}:R26R-miR302–367$^{Tg/+}$ hearts (fig. S5B).

To determine whether the myocardial lineage had undergone de-differentiation and sarcomeric disassembly by miR302–367 overexpression, we lineage-traced the Myh6^{mercremer}:R26R-miR302–367$^{Tg/+}$ line and observed disorganized sarcomeres and reduced sarcomeric gene expression in the Myh6 myocardial lineage positive cells (fig. S5C). Together, these findings demonstrate that persistent expression of miR302–367 in the adult heart reactivates the cardiomyocyte cell cycle and increases cardiomyocyte regeneration. However, such a persistent stimulus leads to induction of a dedifferentiated phenotype and organ-wide dysfunction leading to heart failure.

Transient miR302-mimic therapy promotes cardiac regeneration and improves function after injury

To examine whether transient miR302–367 expression could overcome the adverse effects of persistent expression on the heart, we treated adult mice with miRNA mimics for miR302–367. We first evaluated whether tail-vein injection of miR302b/c/367 mimics led to accumulation of these miRNAs in the heart. miR302b/c/367 mimic levels peaked between 4 and 8 hours after injection and returned to baseline 24 hours after injection (fig. S6A). We observed a similar transient expression of miR302b/c/367 in other organs, including the lung (fig. S7A). For subsequent experiments, we used only miR302b/c mimics because these

miRNAs target Hippo signaling components both in our studies (fig. S3G and table S3) and in a previous study (24).

We administered miR302b/c mimics or a negative control mimic daily for 7 days by tail-vein injections. The expression of miR302-targeted genes related to the Hippo pathway, including *Mst1*, *Lats2*, and *Mob1b*, were decreased in the hearts of miR302b/c mimic–treated mice (fig. S6B). Expression of genes associated with cardiomyocyte differentiation and proliferation were examined at an early time point (day 8) and late time point (day 21) after mimic treatment. The expression of the proliferation-associated gene *Ccnd1* increased at day 8, but returned to basal levels at day 21 (fig. S6C). The expression of *Nppa* and the ratio of *Myh6* to *Myh7* expression were also altered at day 8, but returned to normal levels at day 21 (fig. S6C).

Next, we treated adult mice with miR302b/c mimics or a negative control miRNA mimic, using daily tail-vein injections starting 1 day after MI and continuing daily for 7 days. The expression of the Hippo signaling components *Mst1* and *Mob1b* was significantly decreased in miR302b/c mimic–treated hearts after MI compared to the controls (fig. S6D). Forty-eight hours after the final treatment, we observed increased cardiomyocyte proliferation and decreased apoptosis in the hearts of miR302b/c mimic–treated mice (fig. S6E). On the final treatment day (day 8 after MI), there was a significant increase in the expression of genes associated with cell proliferation (*Ccnd1*), antiapoptosis (*Bcl2*), and fetal gene program (*Nppa, Myh7*) in miR302b/c mimic–treated hearts; however, expression returned to basal levels 4 weeks after surgery (fig. S6F). This ratio of Myh6 to Myh7 expression, which was decreased at 8 days, was increased at 4 weeks (fig. S6F), suggesting transient de-differentiation of cardiomyocytes in miR302b/c mimic–treated hearts.

Analysis of miR302b/c mimic–treated hearts 50 days after injury showed that they also had significantly less fibrotic scarring than the control mimic–treated hearts (Fig. 7, A to C). Functional assessment of miR302b/c mimic–treated animals showed that they exhibited significantly increased fractional shortening and ejection fraction after injury compared with the control mimic–treated animals but did not reach the ejection fraction and fractional shortening of sham animals (Fig. 7D). miR302b/c mimic–treated mice displayed reduced cardiac remodeling, as gauged by end-diastolic volume and end-systolic volume measurements (Fig. 7E). Moreover, miR302b/c mimics increased the density of new blood vessels in the peri-infarct zone but did not affect vascular cell proliferation (fig. S6, G to I). We did not observe abnormalities in other organs, including the lung, liver, and intestine, in miR302b/c mimic–treated mice at 50 days after MI (6 weeks after final treatment), suggesting no adverse effects (fig. S7B). Together, these data indicate that transient expression of miR302 mimics resulted in improved cardiac repair and regeneration after MI.

DISCUSSION

Although various cell therapies have been proposed for cardiac regeneration or treatment of heart failure, several clinical trials have indicated limited efficacy in such strategies [reviewed in (25)]. An alternative approach is to promote endogenous cardiomyocyte proliferation to regenerate and repair the heart, both after injury and in chronic disease

states. Although previous studies have detected a very low level of postnatal cardiomyocyte proliferation in the mouse and human heart (4), it is insufficient to promote cardiac repair and regeneration after injury in mammals. Pathways that can be harnessed to promote cardiomyocyte proliferation would be ideal targets for new therapeutic approaches for cardiac regeneration in humans. miRNAs have emerged as important regulators of and possible therapeutic targets in cardiovascular disease [reviewed in (26)].

Here, we demonstrate that the miR302–367 cluster promotes embryonic and postnatal cardiomyocyte proliferation, in part through targeting multiple kinases in the Hippo signal transduction pathway. Transient treatment of mice with small-molecule miR302 mimics led to improved cardiac regeneration, increased cardiomyocyte proliferation and survival, and improved vessel formation in the peri-infarct region—all accompanied by decreased fibrosis. The reduced fibrotic scarring was likely due to the observed enhancement of myocardial regeneration. In support of this argument, experiments in zebrafish have shown that cardiac injury induces a high level of cardiomyocyte proliferation with a concomitant decrease in fibrotic scarring (27). Additional studies have indicated that cardiomyocytes can inhibit cardiac fibrosis in a paracrine manner (28, 29). These studies provide a framework to explore miRNA mimic–based treatments to promote heart repair and regeneration in humans.

The Hippo pathway regulates proper organ size by regulating cell proliferation as well as programmed cell death. Recent studies have shown that inhibition of Yap phosphorylation through loss of key components in the pathway, such as Salvador/WW45, or expression of a phosphorylation-resistant form of Yap can lead to a profound increase in adult mouse cardiomyocyte proliferation (18). Cardiac-specific loss of Yap leads to increased myocyte apoptosis and fibrosis (30). In our study, miR302–367 targeted multiple components of the Hippo signaling kinase cascade to promote cardiomyocyte proliferation. Our data show that overexpression of miR302–367 promoted cell proliferation while decreasing programmed cell death, consistent with inhibition of Hippo signaling. Moreover, our data show that loss of miR302–367 led to increased phospho-Yap, but decreased nuclear Yap, in $Nkx2.5^{cre}$:$miR302–367^{flox/flox}$ mouse hearts. However, our experiments did not lead to a complete loss of Yap or its function, which likely accounted for the milder phenotype in these mice in comparison to a total loss of Yap (12).

miR302–367 is expressed at high levels in both the developing mouse heart and lung as well as in ES cells, where it plays an important role in promoting pluripotency (6, 8). Other miRNAs have also been shown to promote murine cardiomyocyte proliferation, including miR590 and the miR17–92 family (24, 31). miR17–92 is expressed in the developing mouse heart and lung, and can promote a highly proliferative and un-differentiated state in lung epithelium, similar to miR302–367 (7, 31, 32). As such, certain miRNAs can maintain an undifferentiated state by promoting high levels of cell proliferation while inhibiting differentiation. We show that miRNA mimic strategies can promote cardiac regeneration in vivo in a transient manner that avoids the deleterious effects of persistent cardiomyocyte dedifferentiation.

Previous studies describing overexpression of miR17–92 or YapS127A in mice did not report decreased cardiac function (12, 31). Several reasons could explain the difference between our data and these reports, including a more potent level of overexpression in our studies and additional functions for miR302–367 that were not shared by these other approaches. Regardless of the mechanism, maintaining a persistent high level of cardiomyocyte proliferation could lead to dedifferentiation, directly or indirectly, which could cause compromised contractility and heart failure. Our data also provide a cautionary note that such therapies, if translated, will need to be transient in nature to avoid prolonged cardiac dysfunction from the induction of a dedifferentiated state in proliferating cardiomyocytes.

Our study advances a new approach that delivers a transient proliferative stimulus to the injured heart using a simple methodology based on miRNA mimics. This approach has distinct advantages over cellular therapy because it does not require engraftment of exogenous cells, which has been a significant hurdle in the field of cardiac regeneration. Moreover, the miRNA mimic approach overcomes the potential for persistent cardiomyocyte dedifferentiation owing to its transient nature, which should lead to preserved cardiomyocyte function after ischemic injury. Although we did not observe any effects in other tissues, such a systemic approach of a proliferative stimulus could affect cellular homeostasis in other organs. Local application of miRNA mimics using bioengineered delivery approaches may improve upon systemic administration in the future. Improvement in miRNA mimic chemistry should also allow for precise treatment regimens as well as low potential for off-target affects.

Translation to human cardiac regeneration will require testing of such miRNA mimics first in larger animals whose cardiovascular physiology is more similar than rodents to that of humans, such as pigs. These studies provide an example of a small-molecule miRNA approach to promote cardiac regeneration in situ in mammals. The experience gained from the miRNA antagonists that are already under clinical consideration should greatly accelerate the transition of a mimic approach into human studies.

MATERIALS AND METHODS

Study design

These studies were designed to determine what role the miR302–367 miRNA cluster plays in cardiomyocyte development and regeneration. Mouse genetic models were used to assess both the loss and gain of function of miR302–367 in cardiomyocyte proliferation and differentiation in the developing and adult hearts. Moreover, a method for activating miR302–367 in the adult heart using miRNA mimic–based treatments was used to show that transient increases of these miRNAs can lead to productive cardiomyocyte proliferation, which improves cardiac regeneration after ischemic injury. Assays used to assess cardiomyocyte proliferation included both nuclear division markers (Ki67, PH3), markers of cytokinesis (Aurora B kinase), and direct measurement of cardiomyocyte numbers before and after treatment. Quantification of cardiomyocyte proliferation was performed by at least two blinded individuals. The number of mice per miRNA mimic treatment group was at least six males to give 80% power to detect an effect size of1.8 SDs using a two-group t test

with a 0.05 two-sided significance level. Experiments were reproduced in three to five independent experiments as indicated in the figure legends. This study was not randomized.

Mouse alleles

The miR302–367$^{flox/flox}$ allele was generated by flanking all five of the miRNAs in this cluster with loxP sites using standard homologous recombination in ES cells (33). The R26R-miR302–367$^{Tg/+}$ allele was generated using previously described vectors to insert a DNA sequence containing all five members of the miR302–367 cluster into the CAGR26R locus using standard homologous recombination in ES cells (10, 34). Genotyping primers for these two new alleles are listed in table S5. Generation and genotyping of the Nkx2.5^{cre} and Myh6^{mercremer} lines has been described previously (9, 35, 36). Mice were kept on a mixed C57BL/6:129SVJ background. The experimental MI procedure is described in Supplementary Materials and Methods. All animal procedures were performed in accordance with the Institutional Animal Care and Use Committee at the University of Pennsylvania.

Neonatal cardiomyocyte isolation and culture

Neonatal mouse cardiomyocytes were prepared by the Cardiac Myocyte Core Laboratory at the University of Pennsylvania. Briefly, mouse cardiomyocytes were isolated by enzymatic disassociation of 1-day-old neonate hearts (P1). Cells were plated differentially for 2 hours to remove fibroblasts. Cardiomyocytes were plated on laminin-coated glass coverslips (10 μg/cm^2)in12-well plates at 2.5×10^{5}cells per well. On the following day, culture medium was replaced with fresh medium, and the cells were transduced with miR-302–367 lentivirus (37) and Yap shRNA lentivirus (pLKO.1-Yap shRNA) (Thermo Scientific Open Biosystems, RMM4534), using polybrene (5 mg/ml; American Bioanalytical). After 48 hours, cardiomyocytes were fixed and processed for immunostaining with the indicated antibodies.

Lentivirus expression in cardiomyocytes

Human embryonic kidney (HEK) 293T cells (American Type Culture Collection) were cultured on 100-mm plates at 70% confluence. Lentiviral vectors were packaged in 293T cells using X-tremeGENE9 (Roche) to deliver 5 mg of the lentiviral plasmid, 2.5 μg of psPAX2, and 2.5 μg of pMD2.G (Addgene plasmid 12259). Viral supernatant was collected at 48 hours after transfection, concentrated, and applied to cardiomyocytes.

Adult cardiomyocyte isolation and FACS analysis

Adult hearts (8 to 10 weeks old) were dissected. Ventricular myocytes were isolated using a modified method of a previously described protocol (38). Briefly, excised hearts were mounted on a Langendorf apparatus and perfused with Ca^{2+}-free Tyrode's solution for 6 min at3.0 to 3.5 ml/min at a temperature of 37°C, followed by 12 to 15 min of perfusion with Ca^{2+}-free Tyrode's solution containing collagenase B(0.35 mg/ml), collagenase D (0.25 mg/ml; Roche Chemical Co.), and protease type XIV (0.05 mg/ml; Sigma Chemical Co.). The ventricles were teased into small pieces with forceps, and sections of ventricular tissue were gently triturated with a Pasteur pipette to dissociate individual myocytes. Noncardiomyocytes were depleted by centrifugation. Cardiomyocyte suspension was rinsed

with phosphate-buffered saline (PBS) and then fixed in intracellular fixation buffer (eBioscience). For FACS analyses of cardiomyocyte purity, cells were first permeabilized in 1× permeabilization buffer (eBioscience) and then incubated with cardiac troponin T (1:100; Thermo Scientific, MS-295-P1) for 2 hours at room temperature, followed by incubation with secondary antibody (Alexa Fluor 647, Life Technologies) for 1 hour at room temperature. Samples were analyzed on a BD FACSCanto II (BD Biosciences).

Systemic delivery of miRNA mimics using a neutrallipid emulsion

Synthetic miR302b/c mimics and miRNA mimic control (Dharmacon) were formulated with Neutral Lipid Emulsion (NLE, MaxSuppressor in vivo RNALancerII, BIOO Scientific) according to the manufacturer's instructions. Adult mice (10 weeks) were given a single dose of 10-μg NLE-formulated miRNA mimics by intravenous tail-vein injection. A single dose per day was chosen on the basis of studies showing that the half-life of the mimics in cardiac tissue was between 8 and 24 hours (fig. S6A). Hearts were perfused with PBS to remove circulating blood and snap-frozen in liquid nitrogen at the indicated time points after miRNA mimic treatment. For qRT-PCR of mimic concentration in tissue, RNA was isolated from the heart tissues following the mirVana miRNA Isolation Kit procedure (Ambion). To determine the effect of miRNA mimics on cardiovascular outcome after MI, miR-302b/c mimics or miRNA mimic control (10 μg per mouse systemically) was administered daily for 7 days after MI.

Western blot analysis

Proteins were isolated and solubilized after TRIzol extraction of RNA and DNA from cultured cells as previous described (39). Briefly, neo natal mouse cardiomyocytes were homogenized in TRIzol reagent, followed by the addition of chloroform. The RNA in the upper, aqueous phase was separated with the DNA and proteins in the lower, organic phase. The DNA was precipitated by the addition of ethanol. The protein in the phenol-ethanol supernatant was precipitated with acetone. The protein pellet was then washed with 0.3 M guanidine hydrochloride/95% ethanol and dissolved in 1% SDS at 50°C. Protein concentrations were determined using the BCA Protein Assay Reagent kit (Bio-Rad Laboratories). Proteins extracts were analyzed on polyacrylamide gels (10% NuPAGE bistris gel, Invitrogen) and transferred onto nitrocellulose membranes (Bio-Rad Laboratories). Rabbit anti-Yap (1:500; Cell Signaling Technology) and mouse anti–glyceraldehyde-3-phosphate dehydrogenase (1:1000; Sigma) were used as the primary antibodies. The blots were detected with SuperSignal West Pico Chemiluminescent Substrate (Thermo Scientific).

High-throughput sequencing of RNA isolated by cross-linking immunoprecipitation

HITS-CLIP was performed as published using the monoclonal argonaute antibody 2A8 (16). Three million mouse ES cells were plated and, 48 hours later, cross-linked once with 400 mJ/cm^2 and an additional 200 mJ/cm^2 on ice. The Illumina library was sequenced on an Illumina GA-IIx at University of Pennsylvania Functional Genomics Core. Reads were aligned to the mouse genome (mm9), RefSeqs, and pre-miRNA (mirBase 13.0) using ELAND and allowing up to two mismatches. Significant CLIP tag cluster peaks located in the 3′UTR of mRNAs were identified, and potential miRNA regulators were identified as previously described (40).

Statistics

Data are reported as means ± SEM of at least three independent assays unless otherwise noted. Unpaired Student's *t* test was used to for single comparisons, and one-way ANOVA for multiple comparisons. Statistical significance is displayed as $*P < 0.05$ or $**P < 0.01$ unless indicated otherwise.

Supplementary Material

Refer to Web version on PubMed Central for supplementary material.

Acknowledgments:

We thank the members of the Histology Core in the Penn Cardiovascular Institute for their exemplary work in these studies. We are also thankful to B. Stanger for providing Yap shRNA lentiviral plasmids, Z. Mourelatos for providing the argonaute-2 antibody, K. Margulies for help with neonatal mouse cardiomyocytes isolation, K. Kaestner for help with HITS-CLIP, J. Schug for help with HITS-CLIP bioinformatics analysis, and M. Muniswamy for help with confocal microscopy.

Funding: Supported by grants from the NIH to E.E.M. (R01-HL064632, R01-HL087825, and U01-HL100405) and an NIH K99/R00 grant to Y.T. (K99/R00-HL111348).

REFERENCES AND NOTES

1. Laflamme MA, Murry CE, Heart regeneration. Nature 473, 326–335 (2011). [PubMed: 21593865]
2. Porrello ER, Mahmoud AI, Simpson E, Hill JA, Richardson JA, Olson EN, Sadek HA, Transient regenerative potential of the neonatal mouse heart. Science 331, 1078–1080 (2011). [PubMed: 21350179]
3. Porrello ER, Mahmoud AI, Simpson E, Johnson BA, Grinsfelder D, Canseco D, Mammen PP,Rothermel BA, Olson EN, Sadek HA, Regulation of neonatal and adult mammalian heart regeneration by the miR-15 family. Proc. Natl. Acad. Sci. U.S.A 110, 187–192 (2013). [PubMed: 23248315]
4. Senyo SE, Steinhauser ML, Pizzimenti CL, Yang VK, Cai L, Wang M, Wu TD,Guerquin-Kern JL, Lechene CP, Lee RT, Mammalian heart renewal by pre-existing cardiomyocytes. Nature 493, 433–436 (2013). [PubMed: 23222518]
5. Gladka MM, da Costa Martins PA, De Windt LJ, Small changes can make a big difference—MicroRNA regulation of cardiac hypertrophy. J. Mol. Cell. Cardiol 52, 74–82 (2012). [PubMed: 21971075]
6. Barroso-delJesus A, Romero-Lopez C, Lucena-Aguilar G, Melen GJ, Sanchez L, Ligero G,Berzal-Herranz A, Menendez P, Embryonic stem cell-specific miR302–367cluster: Human gene structure and functional characterization of its core promoter. Mol. Cell. Biol 28, 6609–6619 (2008). [PubMed: 18725401]
7. Tian Y, Zhang Y, Hurd L, Hannenhalli S, Liu F, Lu MM, Morrisey EE, Regulation of lung endoderm progenitor cell behavior by miR302/367. Development 138, 1235–1245 (2011). [PubMed: 21350014]
8. Card DA, Hebbar PB, Li L, Trotter KW, Komatsu Y, Mishina Y, Archer TK, Oct4/Sox2-regulated miR-302 targets cyclin D1 in human embryonic stem cells. Mol. Cell. Biol 28, 6426–6438 (2008). [PubMed: 18710938]
9. Moses KA, DeMayo F, Braun RM, Reecy JL, Schwartz RJ, Embryonic expression of an Nkx2–5/Cre gene using ROSA26 reporter mice. Genesis 31, 176–180 (2001). [PubMed: 11783008]
10. Tuveson DA, Shaw AT, Willis NA, Silver DP, Jackson EL, Chang S, Mercer KL, Grochow R,Hock H, Crowley D, Hingorani SR, Zaks T, King C, Jacobetz MA, Wang L, Bronson RT,Orkin SH, DePinho RA, Jacks T, Endogenous oncogenic *K-ras*^{G12D} stimulates proliferation and widespread neoplastic and developmental defects. Cancer Cell 5, 375–387 (2004). [PubMed: 15093544]

11. Ikenishi A, Okayama H, Iwamoto N, Yoshitome S, Tane S, Nakamura K, Obayashi T, Hayashi T,Takeuchi T, Cell cycle regulation in mouse heart during embryonic and postnatal stages. Dev. Growth Differ 54, 731–738 (2012). [PubMed: 22957921]
12. Xin M, Kim Y, Sutherland LB, Murakami M, Qi X, McAnally J, Porrello ER, Mahmoud AI,Tan W, Shelton JM, Richardson JA, Sadek HA, Bassel-Duby R, Olson EN, Hippo pathway effector Yap promotes cardiac regeneration. Proc. Natl. Acad. Sci. U.S.A 110, 13839–13844 (2013). [PubMed: 23918388]
13. Mahmoud AI, Kocabas F, Muralidhar SA, Kimura W, Koura AS, Thet S, Porrello ER,Sadek HA, Meis1 regulates postnatal cardiomyocyte cell cycle arrest. Nature 497, 249–253 (2013). [PubMed: 23594737]
14. Zhang Y, Li TS, Lee ST, Wawrowsky KA, Cheng K, Galang G, Malliaras K, Abraham MR,Wang C, Marban E, Dedifferentiation and proliferation of mammalian cardiomyocytes. PLOS One 5, e12559 (2010). [PubMed: 20838637]
15. Vukusic K, Jonsson M, Brantsing C, Dellgren G, Jeppsson A, Lindahl A, Asp J, High density sphere culture of adult cardiac cells increases the levels of cardiac and progenitor markers and shows signs of vasculogenesis. Biomed. Res. Int 2013, 696837 (2013). [PubMed: 23484142]
16. Chi SW, Zang JB, Mele A, Darnell RB, Argonaute HITS-CLIP decodes microRNA–mRNA interaction maps. Nature 460, 479–486 (2009). [PubMed: 19536157]
17. Enright AJ, John B, Gaul U, Tuschl T, Sander C, Marks DS, MicroRNA targets in Drosophila. Genome Biol 5, R1 (2003). [PubMed: 14709173]
18. Heallen T, Zhang M, Wang J, Bonilla-Claudio M, Klysik E, Johnson RL, Martin JF, Hippo pathway inhibits Wnt signaling to restrain cardiomyocyte proliferation and heart size. Science 332, 458–461 (2011). [PubMed: 21512031]
19. Hong W, Guan KL, The YAP and TAZ transcription co-activators: Key downstream effectors of the mammalian Hippo pathway. Semin. Cell Dev. Biol 23, 785–793 (2012). [PubMed: 22659496]
20. Xin M, Kim Y, Sutherland LB, Qi X, McAnally J, Schwartz RJ, Richardson JA, Bassel-Duby R,Olson EN, Regulation of insulin-like growth factor signaling by Yap governs cardiomyocyte proliferation and embryonic heart size. Sci. Signal 4, ra70 (2011). [PubMed: 22028467]
21. Lin Z, von Gise A, Zhou P, Gu F, Ma Q, Jiang J, Yau AL, Buck JN, Gouin KA, van Gorp PR,Zhou B, Chen J, Seidman JG, Wang DZ, Pu WT, Cardiac-specific YAP activation improves cardiac function and survival in an experimental murine MI model. Circ. Res 115, 354–363 (2014). [PubMed: 24833660]
22. von Gise A, Lin Z, Schlegelmilch K, Honor LB, Pan GM, Buck JN, Ma Q, Ishiwata T, Zhou B,Camargo FD, Pu WT, YAP1, the nuclear target of Hippo signaling, stimulates heart growth through cardiomyocyte proliferation but not hypertrophy. Proc. Natl. Acad. Sci. U.S.A 109, 2394–2399 (2012). [PubMed: 22308401]
23. Cox EJ, Marsh SA, A systemic review of fetal genes as biomarkers of cardiac hypertrophy in rodent models of diabetes. PLOS One 9, e92903 (2014). [PubMed: 24663494]
24. Eulalio A, Mano M, Dal Ferro M, Zentilin L, Sinagra G, Zacchigna S, Giacca M,Functional screening identifies miRNAs inducing cardiac regeneration. Nature 492, 376–381 (2012). [PubMed: 23222520]
25. Sanganalmath SK, Bolli R, Cell therapy for heart failure: A comprehensive overview of experimental and clinical studies, current challenges, and future directions. Circ. Res 113, 810–834 (2013). [PubMed: 23989721]
26. Olson EN, MicroRNAs as therapeutic targets and biomarkers of cardiovascular disease. Sci. Transl. Med 6, 239ps3 (2014).
27. Gonzalez-Rosa JM, Martin V, Peralta M, Torres M, Mercader N, Extensive scar formation and regression during heart regeneration after cryoinjury in zebrafish. Development 138, 1663–1674 (2011). [PubMed: 21429987]
28. Nagalingam RS, Sundaresan NR, Noor M, Gupta MP, Solaro RJ, Gupta M,Deficiency of cardiomyocyte-specific microRNA-378 contributes to the development of cardiac fibrosis involving a transforming growth factor β (TGFβ1)-dependent paracrine mechanism. J. Biol. Chem 289, 27199–27214 (2014). [PubMed: 25104350]

29. Tian Y, Morrisey EE, Importance of myocyte-nonmyocyte interactions in cardiac development and disease. Circ. Res 110, 1023–1034 (2012). [PubMed: 22461366]

30. Del Re DP, Yang Y, Nakano N, Cho J, Zhai P, Yamamoto T, Zhang N, Yabuta N, Nojima H,Pan D, Sadoshima J, Yes-associated protein isoform 1 (Yap1) promotes cardiomyocyte survival and growth to protect against myocardial ischemic injury. J. Biol. Chem 288, 3977–3988 (2013). [PubMed: 23275380]

31. Chen J, Huang ZP, Seok HY, Ding J, Kataoka M, Zhang Z, Hu X, Wang G, Lin Z, Wang S,Pu WT, Liao R, Wang DZ, mir-17–92 cluster is required for and sufficient to induce cardiomyocyte proliferation in postnatal and adult hearts. Circ. Res 112, 1557–1566 (2013). [PubMed: 23575307]

32. Lu Y, Thomson JM, Wong HY, Hammond SM, Hogan BL, Transgenic over-expression of the microRNA miR-17–92 cluster promotes proliferation and inhibits differentiation of lung epithelial progenitor cells. Dev. Biol 310, 442–453 (2007). [PubMed: 17765889]

33. Liu P, Jenkins NA, Copeland NG, A highly efficient recombineering-based method for generating conditional knockout mutations. Genome Res 13, 476–484 (2003). [PubMed: 12618378]

34. Wu SP, Lee DK, Demayo FJ, Tsai SY, Tsai MJ, Generation of ES cells for conditional expression of nuclear receptors and coregulators in vivo. Mol. Endocrinol 24, 1297–1304 (2010). [PubMed: 20382891]

35. Sohal DS, Nghiem M, Crackower MA, Witt SA, Kimball TR, Tymitz KM, Penninger JM,Molkentin JD, Temporally regulated and tissue-specific gene manipulations in the adult and embryonic heart using a tamoxifen-inducible Cre protein. Circ. Res 89, 20–25 (2001). [PubMed: 11440973]

36. Agah R, Frenkel PA, French BA, Michael LH, Overbeek PA, Schneider MD,Gene recombination in postmitotic cells. Targeted expression of Cre recombinase provokes cardiac-restricted, site-specific rearrangement in adult ventricular muscle in vivo. J. Clin. Invest 100, 169–179 (1997). [PubMed: 9202069]

37. Anokye-Danso F, Trivedi CM, Juhr D, Gupta M, Cui Z, Tian Y, Zhang Y, Yang W, Gruber PJ,Epstein JA, Morrisey EE, Highly efficient miRNA-mediated reprogramming of mouse and human somatic cells to pluripotency. Cell Stem Cell 8, 376–388 (2011). [PubMed: 21474102]

38. Mitra R, Morad M, A uniform enzymatic method for dissociation of myocytes from hearts and stomachs of vertebrates. Am. J. Physiol 249, H1056–H1060 (1985). [PubMed: 2998207]

39. Hummon AB, Lim SR, Difilippantonio MJ, Ried T, Isolation and solubilization of proteins after TRIzol extraction of RNA and DNA from patient material following prolonged storage. Biotechniques 42, 467–470 (2007). [PubMed: 17489233]

40. Schug J, McKenna LB, Walton G, Hand N, Mukherjee S, Essuman K, Shi Z, Gao Y, Markley K,Nakagawa M, Kameswaran V, Vourekas A, Friedman JR, Kaestner KH, Greenbaum LE, Dynamic recruitment of microRNAs to their mRNA targets in the regenerating liver. BMC Genomics 14, 264 (2013). [PubMed: 23597149]

41. Zhang Y, Goss AM, Cohen ED, Kadzik R, Lepore JJ, Muthukumaraswamy K, Yang J,DeMayo FJ, Whitsett JA, Parmacek MS, Morrisey EE, A Gata6-Wnt pathway required for epithelial stem cell development and airway regeneration. Nat. Genet 40, 862–870 (2008). [PubMed: 18536717]

42. Stypmann J, Engelen MA, Troatz C, Rothenburger M, Eckardt L, Tiemann K, Echocardiographic assessment of global left ventricular function in mice. Lab. Anim 43, 127–137 (2009). [PubMed: 19237453]

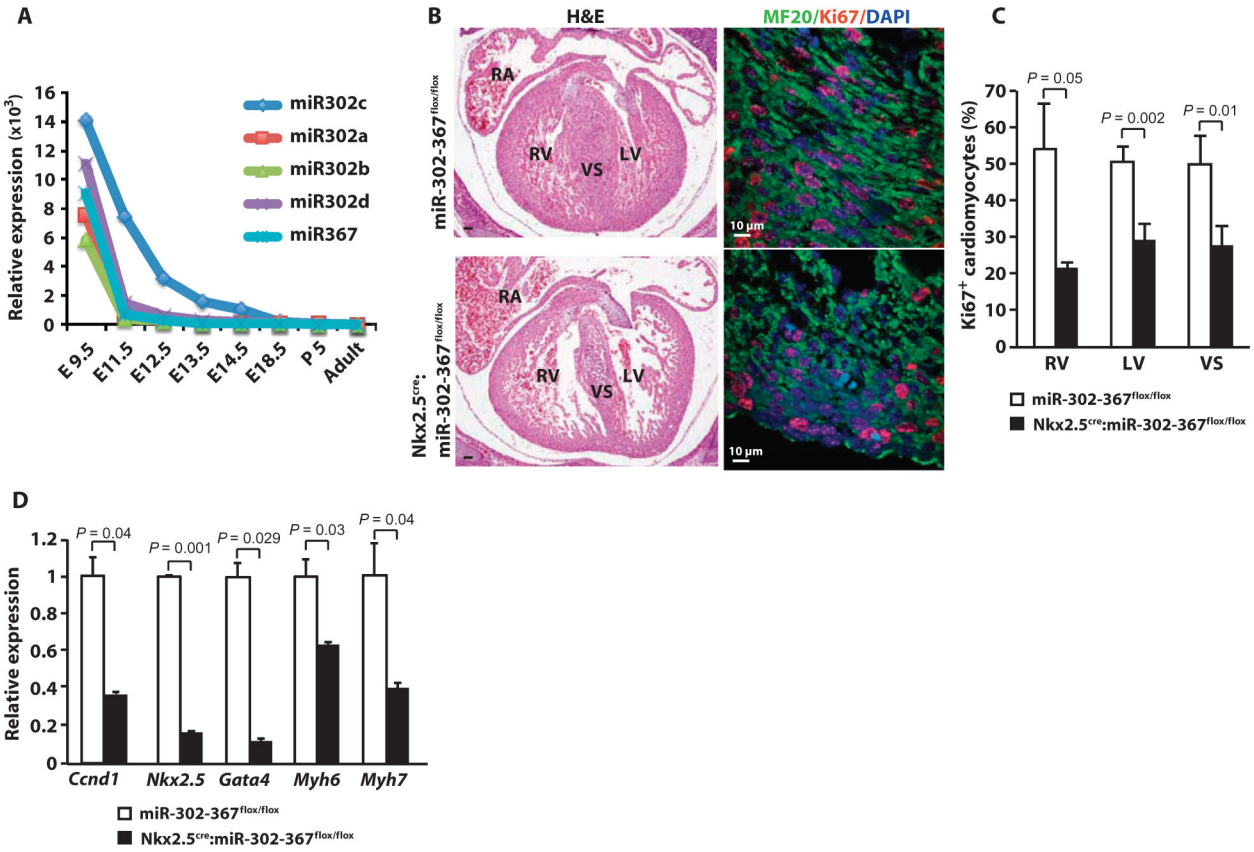

Fig. 1. miR302–367 is expressed in the early heart and is important for cardiomyocyte proliferation.

(A) Relative expression of miR302–367 cluster members during heart development as determined by qRT-PCR. (B) Hematoxylin and eosin (H&E)–stained and immunostained sections of control E14.5 hearts showing thinning of ventricular wall, hypoplastic ventricular septum, and reduced cardiomyocyte proliferation in Nkx2.5^{cre}:miR302–367$^{flox/flox}$ mutants compared with miR302–367$^{flox/flox}$ mice. RV, right ventricle; LV, left ventricle; VS, ventricular septum; RA, right atrium. (C) Quantification of Ki67 (proliferation) from images in (B). (D) Gene expression changes associated with cardiomyocyte proliferation and differentiation in Nkx2.5^{cre}:miR302–367$^{flox/flox}$ null mutants versus controls at E14.5. (C and D) Data are means ± SEM ($n = 3$). *P* values determined by Student's *t* test.

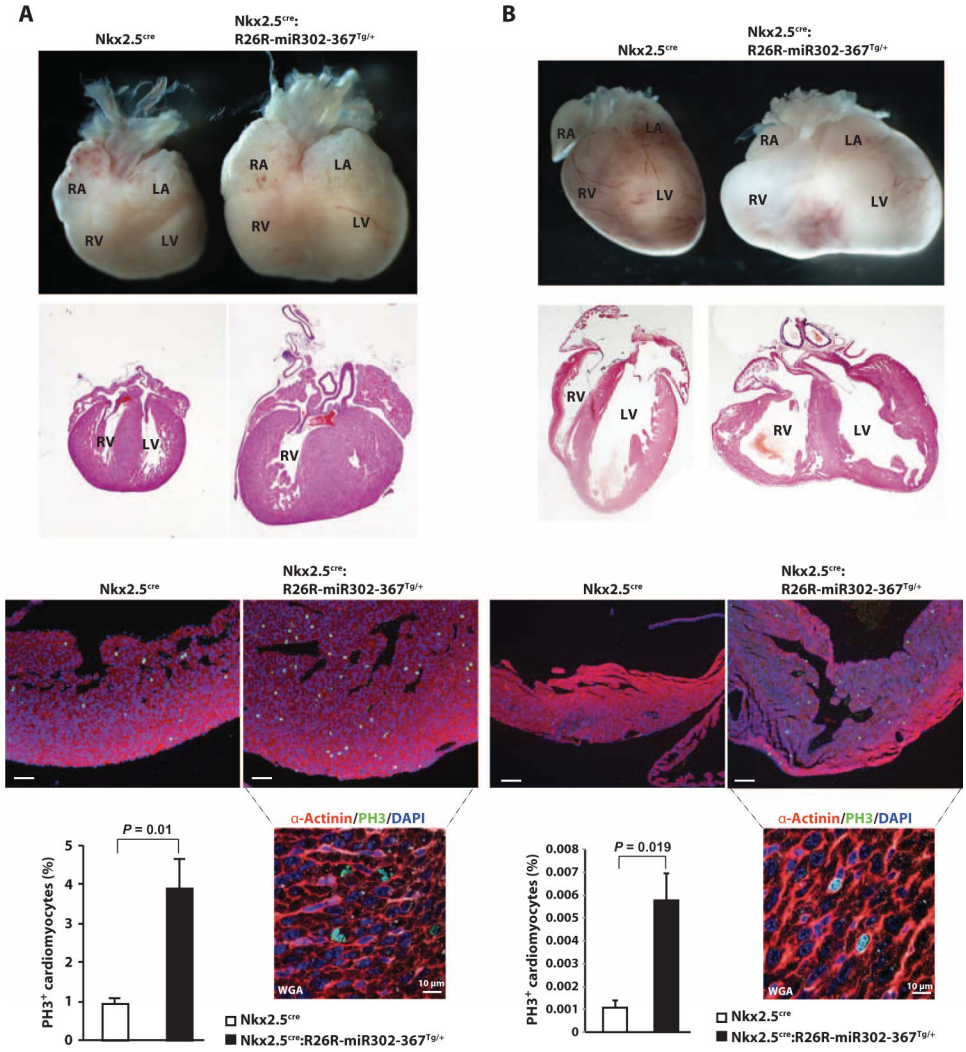

Fig. 2. Overexpression of miR302–367 cluster in the developing heart results in increased cardiomyocyte proliferation and cardiomegaly.

(**A**) At E18.5, Nkx2.5^{cre}:R26R-miR302–367$^{Tg/+}$ mutants have an enlarged heart with thickened ventricular myocardium and ventricular septal defects compared to Nkx2.5^{cre} controls. (**B**) Cardiomegaly and increased cardiomyocyte proliferation in Nkx2.5^{cre}:R26R-miR302–367$^{Tg/+}$ mutant hearts at P20. (A and B) Immunostainings for PH3 and a-actinin and wheat germ agglutinin (WGA) show the number of mitotic cardiomyocytes. Scale bars, 100 mm. High-magnification reveals PH3^{+} cardiomyocytes. LA, left atrium. Data are means ± SEM (n = 3). P values determined by Student's t test.

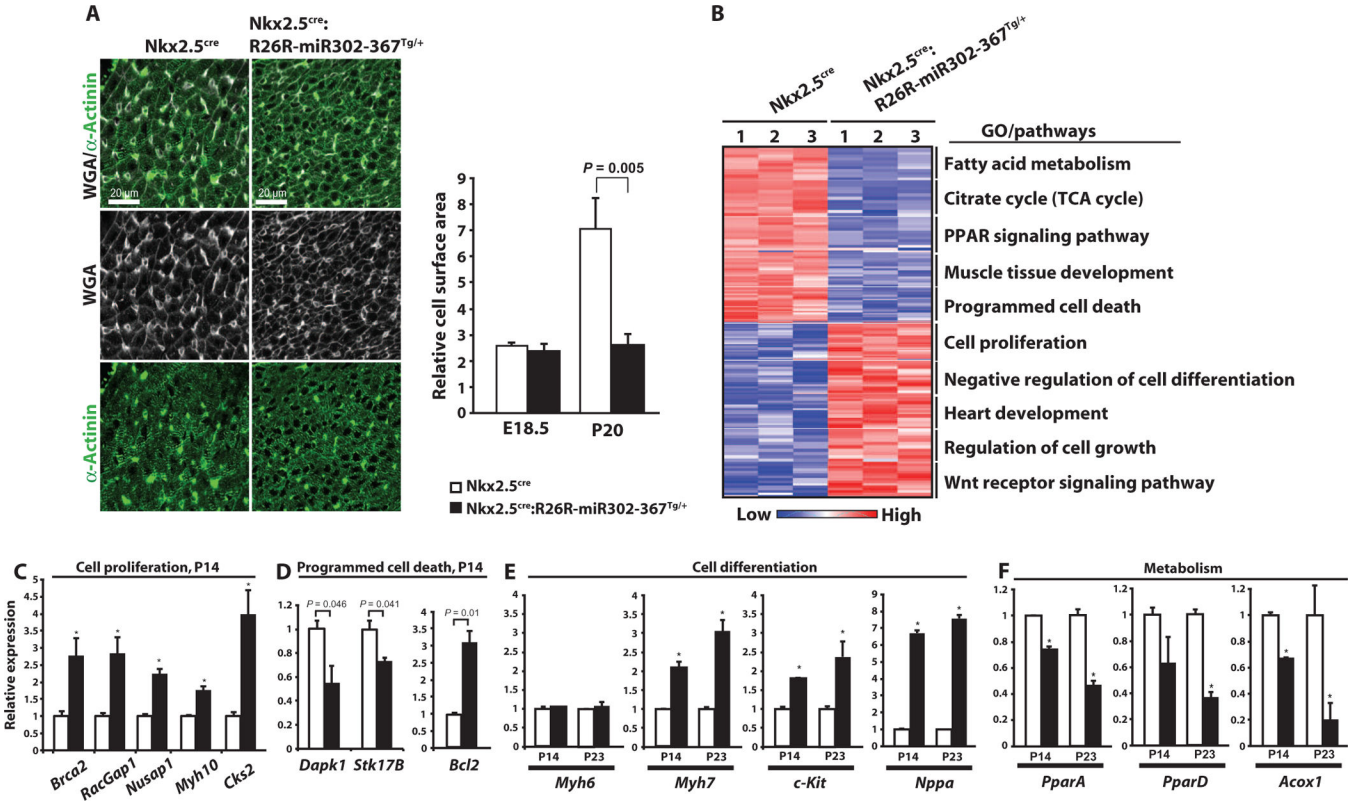

Fig. 3. miR302–367 overexpression leads to increased cell proliferation as well as altered differentiation and metabolism in cardiomyocytes.

(**A**) Wheat germ agglutinin and a-actinin staining of hearts at P20. Cell surface area was quantified at E18.5 and P20. Quantitative analyses represent counting of five fields from three independent samples per group. (**B**) Heatmap and pathways profile of microarray analysis of Nkx2.5^{cre} and Nkx2.5^{cre}:R26R-miR302–367$^{Tg/+}$ mutant hearts at P14. (**C** and **D**) Gene expression changes related to cell proliferation (C) and programmed cell death (D) at P14. (**E** and **F**) Gene expression changes related to differentiation (E) and fatty acid metabolism (F) at P14 and P23. Data are means ± SEM (n = 3 per group). *P < 0.05 versus Nkx2.5^{cre} control animals (Student's t test).

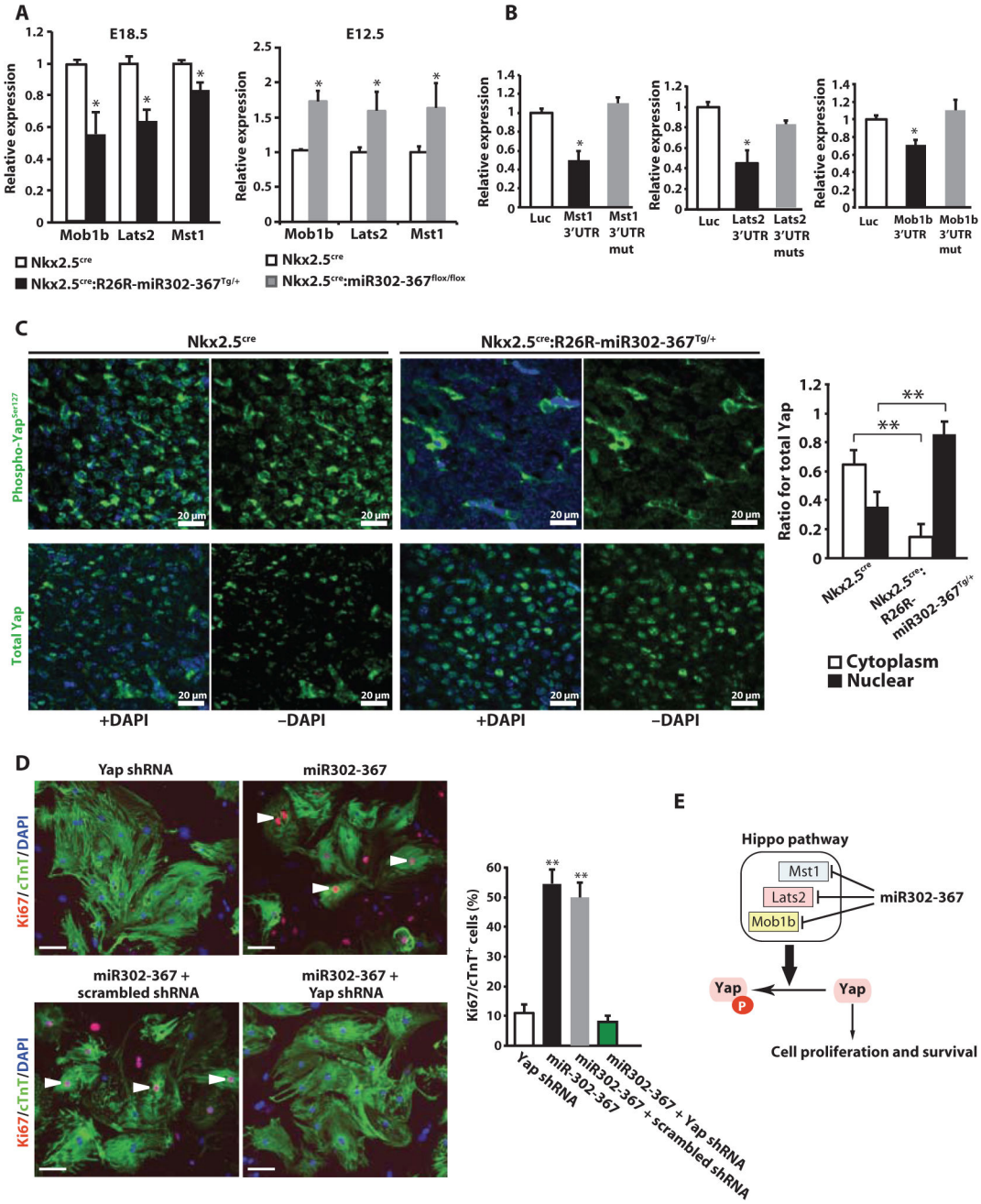

Fig. 4. miR302–367 promotes cardiomyocyte proliferation through regulation of Hippo pathway kinases.

(**A**) Expression of *Mob1b*, *Lats2*, and *Mst1* in Nkx2.5^{cre}:R26R-miR302–367$^{Tg/+}$ mutant hearts at E18.5 and Nkx2.5^{cre}:R26R-miR302–367$^{flox/flox}$ null mutant hearts at E12.5 by qRT-PCR. (**B**) Luciferase reporter assays showing that miR302–367 can repress Mst1, Lats2, and Mob1b expression through their respective 3′UTRs. This repression can be reversed by mutations of the miR302–367 binding sites. (**C**) Confocal fluorescence microscopy of phospho-Yap and nuclear staining of Yap, with or without DAPI, in ventricular cardiomyocytes of Nkx2.5^{cre}:R26R-miR302–367$^{Tg/+}$ mouse hearts at E18.5. Cytoplasmic and nuclear ratio for total Yap protein was quantified using Fiji software. (A to

C) *$P < 0.05$, **$P < 0.01$ versus Nkx2.5^{cre} control hearts (Student's *t* test). (**D**) Overexpression of miR302–367 in primary mouse neonatal cardiomyocytes. Cardiomyocyte proliferation was quantified using Ki67 immunostaining. **$P < 0.01$ versus Yap shRNA control. Scale bars, 100 μm. (**E**) Proposed model of miR302–367 promoting cardiomyocyte proliferation through regulation of Hippo pathway kinases. (A to D) Data are means ± SEM ($n = 3$ for A, C, and D; $n = 5$ for B).

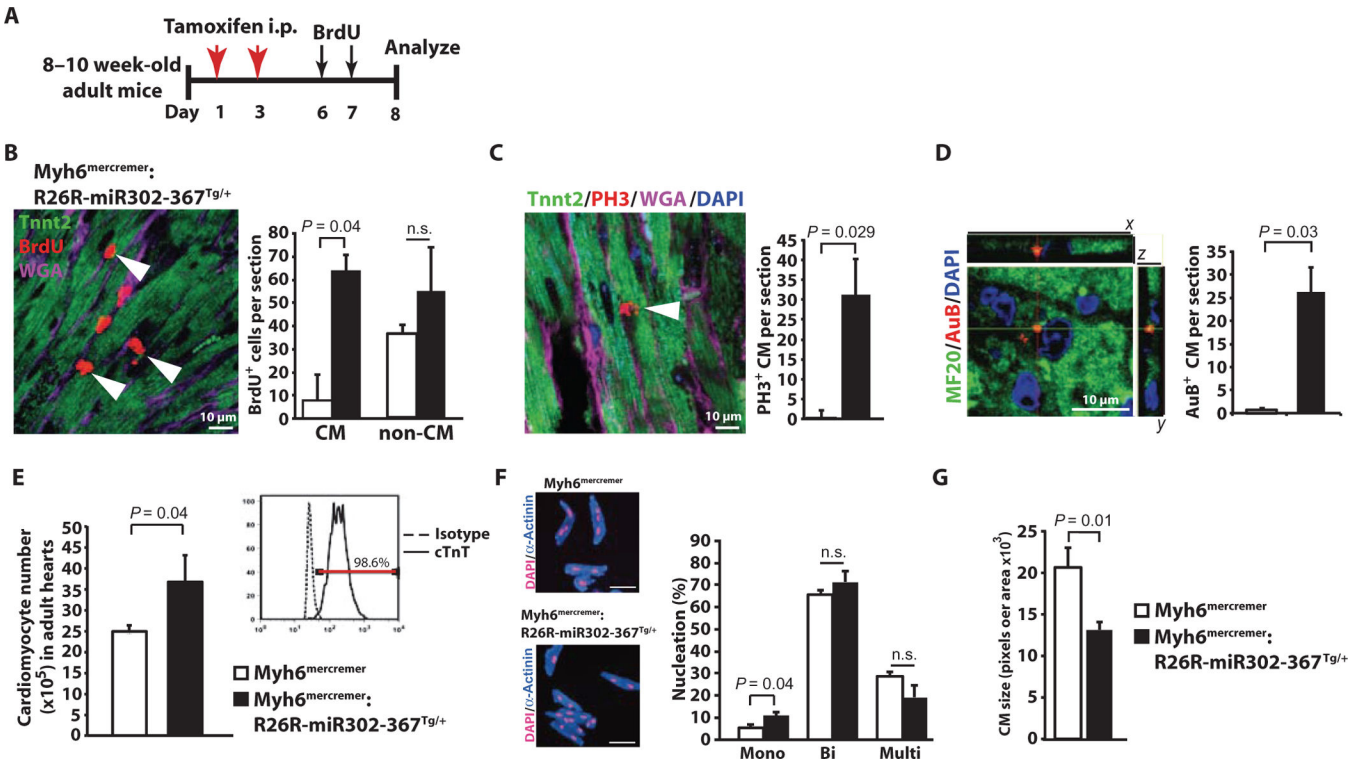

Fig. 5. miR302–367 can promote cardiomyocyte proliferation in the adult heart.

(**A**) Schematic of tamoxifen-inducible miR302–367 overexpression in the hearts of adult Myh6^{mercremer} mice. (**B** to **D**) Confocal images with z-stacking and quantification showing the number of cells reentering the cell cycle [5-bromo-2′-deoxyuridine (BrdU)$^{+}$] (B), undergoing mitosis (PH3^{+})(C), or undergoing cytokinesis [Aurora B (AuB)$^{+}$] (D) 7 days after induction of miR302–367 expression in the adult heart. (**E**) Number of cardiomyocytes in Myh6^{mercremer} and Myh6^{mercremer}:R26R-miR302–367$^{Tg/+}$animals. Inset: Fluorescence-activated cell sorting (FACS) plot shows that 98.6% of the isolated cells counted in the adult hearts are cTnT^{+} cardiomyocytes. (**F**) Number of nuclei in control and Myh6^{mercremer}:R26R-miR302–367$^{Tg/+}$ cardiomyocytes. Scale bars, 100 mm. mono, mononucleated; bi, binucleated; multi, multinucleated About 1 × 10^{3} cardiomyocytes were counted per sample. (**G**) Cell sizes of the isolated cardiomyocytes. Data are means ± SEM (n = 3). P values determined with Student's t test. n.s., no significant change.

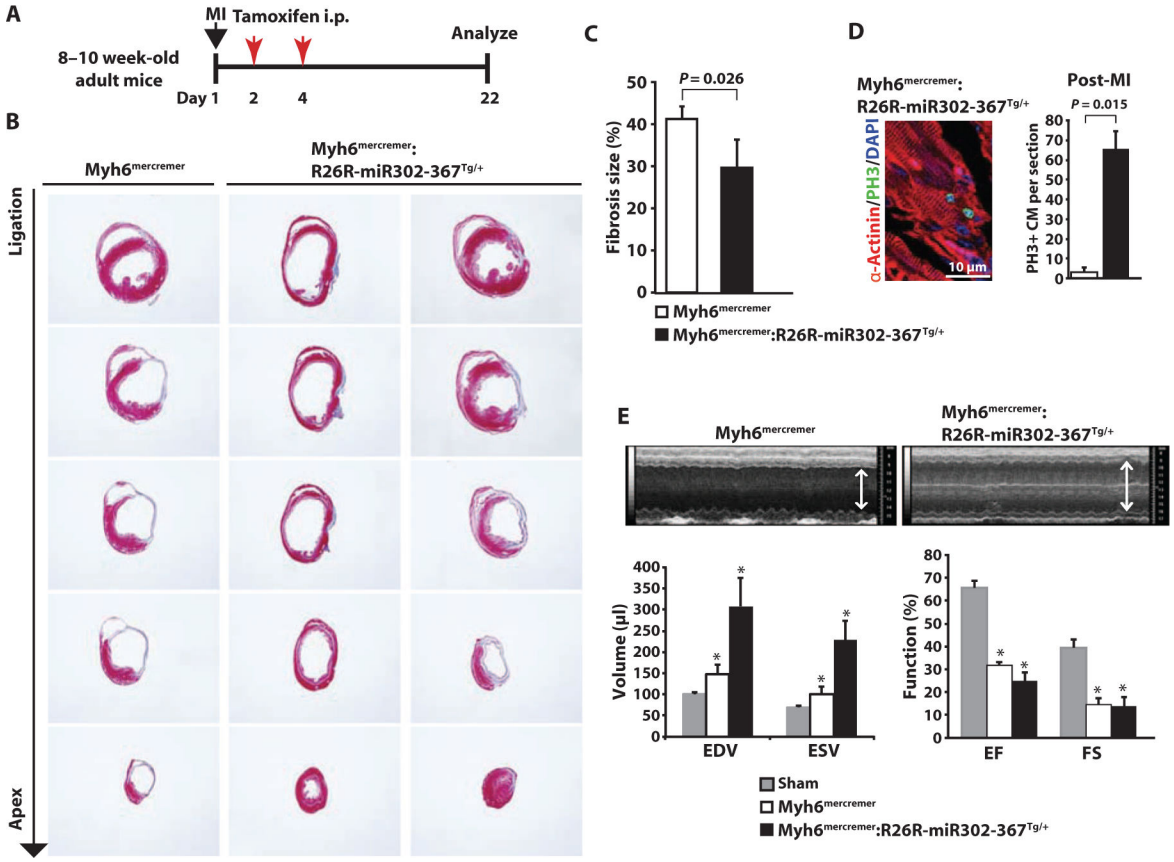

Fig. 6. Prolonged miR302–367 overexpression in the adult heart reduces fibrotic scar size but compromises cardiac function after MI.

(**A**) Study design of miR302–367 overexpression by tamoxifen intraperitoneal injection after MI by ligation of the left anterior descending (LAD) coronary artery. (**B**) Masson's trichrome–stained heart sections from the site of ligation toward the apex of control and Myh6^{mercremer}:R26R-miR302–367$^{Tg/+}$ mice at 21 days after MI. Serial sections were cut at 500-μm intervals from the site of the ligature toward the apex. One representative Myh6^{mercremer} and two Myh6^{mercremer}:R26R-miR302–367$^{Tg/+}$ hearts are shown (n = 6 per group). (**C**) Quantification of the fibrotic regions in heart sections in (B). (**D**) Immunostaining and quantification ofPH3^{+}/α-actinin^{+}cellsinMyh6^{mercremer}and Myh6^{mercremer}:R26R-miR302–367$^{Tg/+}$ hearts at 21 days after MI. (E) Cardiac function in mice subjected to LAD ligation, evaluated by echocardiography (n = 7 per group). EF, ejection fraction; FS, fractional shortening; EDV, end-diastolic volume; ESV, end-systolic volume. Data are means ± SEM (n = 6 to 7). (C and D) P values determined with Student's t test. (E) *P < 0.05 versus sham, by one-way analysis of variance (ANOVA).

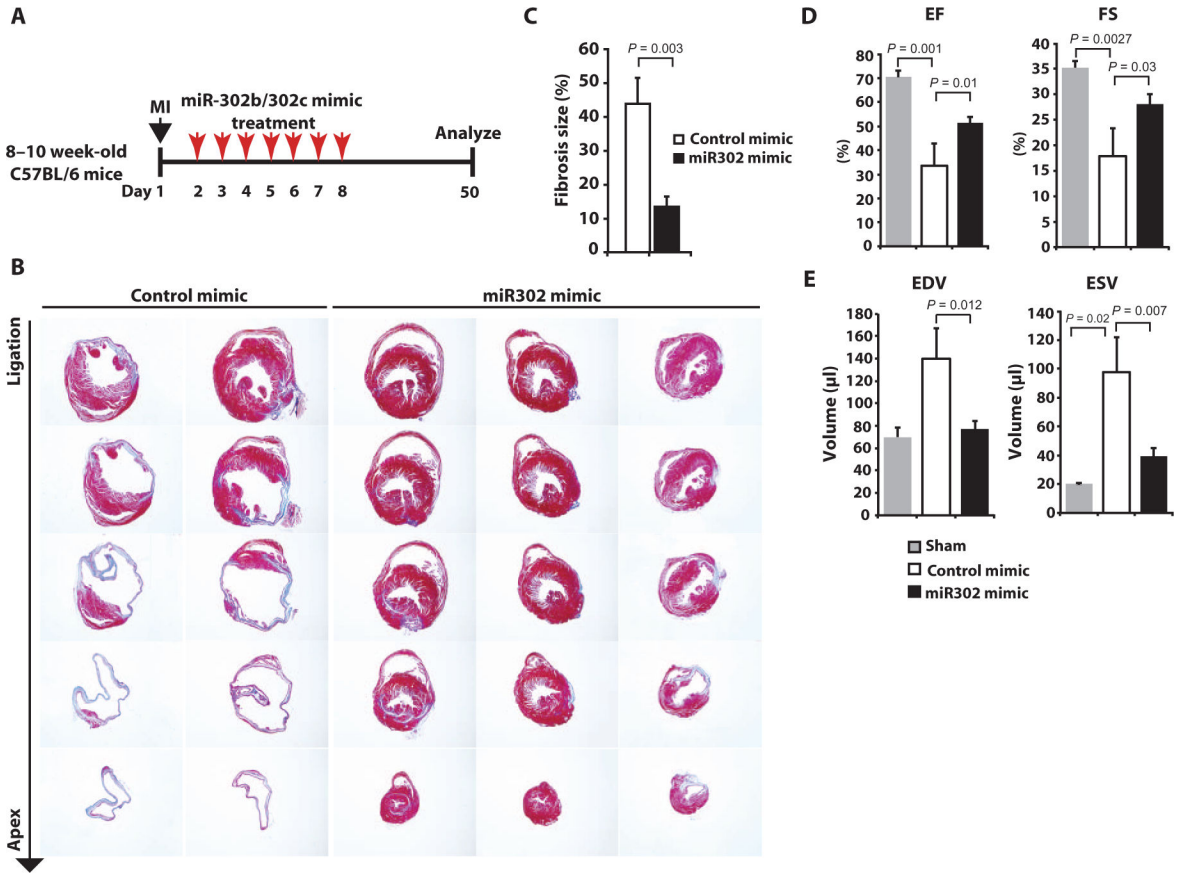

Fig. 7. Transient miR302 mimic therapy promotes cardiac regeneration and improves function of injured hearts.

(**A**) Schematic of 7-day miR302 mimic treatment after MI ($n = 3$ sham; $n = 8$ control; $n = 18$ miR302). (**B**) Masson's trichrome staining of heart sections 50 days after MI and 42 days after final treatment with control or miR302 mimic. Serial sections were cut at 500-μm intervals from the site of the ligature toward the apex. Two representative control and three miR302 mimic–treated hearts are shown. (**C**) Quantification of the fibrotic areas in heart sections. Data are means ± SEM. (**D** and **E**) Cardiac function of mice subjected to LAD ligation was evaluated by echocardiography. Data are means ± SEM. *P* values determined by one-way ANOVA.